FRACTURE ZONE CHARACTERIZATION—MICRO-MECHANICAL STUDY

Svetlana Vasic†

Post-doctoral Research Fellow
Department of Civil and Environmental Engineering
University of Maine
Orono, ME 04469-5711

Ian Smith†

Professor
Faculty of Forestry and Environmental Management
University of New Brunswick
Fredericton, N.B.
Canada E3B 6C2

and

Eric Landis

Associate Professor
Department of Civil and Environmental Engineering
University of Maine
Orono, ME 04469-5711

(Received November 2000)

ABSTRACT

The experimental and numerical characterization of the fracture process zone in softwoods is presented. In-situ real-time Scanning Electron Microscopy (SEM) was used as a tool to examine the physical mechanism of fracture in softwoods (spruce) using end-tapered Double Cantilever Beam specimens. Fracture process zone has been characterized in terms of failure mechanisms. It was found that bridging behind the crack tip is the main toughening mechanism, which contributes to nonlinear wood behavior in the presence of stress concentrations.

Keywords: Fracture mechanics, fracture zone, *in-situ* real-time SEM observations, crack profiles, fiber bridging, toughening.

INTRODUCTION

Since the first successful attempts to apply the theory of fracture mechanics to wood (Attack et al. 1961), various research studies have focused on fracture characterization, test methods, and interpretation of fracture parameters applicable to engineering problems. Fracture mechanics has also provided valuable concepts for evaluation of the influence of crack-like defects, notches, and other stress raisers in structural members and wood-adhesive joints.

The crucial level of characterization of wood fracture behavior is related to the definition of the damage zone ahead of a crack tip. Compared to the body of knowledge about modes of wood failure at the macroscopic level, our perception and understanding of the character and size of the process zone ahead of a major crack tip are rather poor. No research studies (prior to Vasic 2000) have been found in the literature that focused on the delicate task of qualitative and/or quantitative characterization of the fracture zone. Because

† Member of SWST

Wood and Fiber Science, 34(1), 2002, pp. 42–56

of the apparent brittleness of wood, the Linear Elastic Fracture Mechanics (LEFM) approach has commonly been considered as an attractive and promising tool for wood strength predictions and engineering applications. Yet, the LEFM approach holds to a good approximation only when the process zone is small in respect to the crack length or the dimensions of the cracked body. The basic assumptions of the LEFM are, however, often violated. The relatively large volume of literature on the subject of LEFM applications to wood is flooded with rather conflicting and confusing experimental data (Valentin et al. 1991). There seems to be a lack of objectivity and relevance outside the original specific testing configurations. There is a growing body of opinion that wide discrepancies in results are associated with failure mechanisms in the process zone ahead of the crack tip. A process zone is not elastic and not accounted for in the single parameter **K** characterization of the crack-tip stress field (e.g., Bostrom 1992; Yeh and Schniewind 1992; Smith and Chui 1994; Smith and Hu 1994; Vasic and Smith 1996a, b, 1998, 1999; Vasic 2000).

The experience gained through the applications of fracture mechanics to other quasi-brittle materials, e.g., concrete, ceramics, and rocks, has provided the definition of the process zone size as a ". . . measure of the deviation from linear elastic behavior shown by the material" (Atkinson 1987). The macroscopic inelastic behavior is completely controlled by heterogeneities on the 'grain scale' and their interaction under triaxial stress (or strain) induced at the major crack tip. It is therefore, rational to presume that the damage process zone characterization is fundamental to understanding the mechanism of crack growth.

Experimental evidence for the existence of an inelastic process zone ahead of a wood crack can be found throughout the results from different laboratories. Such evidence is most often obscured because parameters varied between investigations. While seeking originality, various investigators have used quite different experimental techniques and testing conditions. Due caution must be exercised in distinguishing the effects of an intrinsic damage zone development from other potential influences.

THE LIMITATIONS OF LEFM APPLIED TO WOOD

The evaluation of the basic parameters of Linear Elastic Fracture Mechanics (LEFM) presumes that the following principles hold:

1. The material is a homogeneous, isotropic (or orthotropic, Sih et al. 1965) linear elastic medium.
2. The preexisting crack always propagates along the original crack direction, i.e., in a self-similar manner.
3. Crack-tip displacements can be separated into three different modes, namely in plane tension, in-plane shear, and out-of-plane shear.
4. The intensity of the corresponding stress distributions in the vicinity of the single crack tip is fully characterized by the stress intensity factors K_I, K_{II}, and K_{III}.
5. The inelastic process zone is confined to a small volume at a crack tip. It has a radius (r) small enough to satisfy the condition $r/a < 0.02$ (**a** is the crack length, or any dimension of the cracked body).
6. Crack surfaces are traction-free at all stages of loading, and the crack tip is anatomically sharp.
7. Once the critical fracture condition (fracture toughness K_c or critical strain energy release rate G_c) has been reached or exceeded, the crack propagates dynamically at some terminal velocity.

In respect to these features of LEFM, fracture behavior of wood may be characterized and compared as follows:

1. Wood is a heterogeneous, approximately cylindrically orthotropic material with discontinuities on both micro- and macrostructural levels. Brittle wood fracture usually occurs while in an elastic range.
2. For all strongly anisotropic materials, the

crack does not necessarily grow along the original crack orientation, e.g., in unidirectional composites the crack always grows along the fibers. In wood the initial crack extension is always parallel to the grain, even when the starter crack lies across the grain (Ashby et al. 1984). Only for the special case of an original crack along the fiber direction, does this deviation from the principles of LEFM vanish. It is likely that the crack in wood never propagates in a strictly self-similar manner, due to heterogeneous and discrete natured micro- and macrostructure. Microscopically, probably with no exception, fractured surfaces are irregular and tortuous.

3. In the terms of the above discussion, it can be concluded that it is only when a crack propagates in a self-similar manner that the displacements determined with the aid of Westergaard's equations are not of mixed mode. Hence, only then can displacements be separated into three independent modes (Knott 1973; Broek 1982).
4. Popularity of fracture mechanics has been associated with the attractiveness of a simple one-parameter K_n (n = I, II, III) description for all complex fracture phenomena that different materials may exhibit. Yet, whenever all the principles of LEFM do not strictly hold for the specific material behavior, the simplicity of K characterization must be sacrificed.
5. The principle of 'smallness' of the inelastic process zone appears to be the most important issue for satisfactory applications of LEFM (Fig. 1). As emphasized previously, this zone in wood (or wood-composite products) has not yet been characterized appropriately, either by experimental observations, or by understanding the failure mechanisms involved.
6. It seems reasonable to speculate that crack surfaces are not traction-free during episodic slow crack growth in wood, and that the crack is not anatomically sharp. It could be further speculated that while the crack is seeking the planes of least resistance, on the microscale it leaves some 'islands' of intact-material behind the advancing fracture front. This mechanism is known as 'ligamentary bridging.' No matter the type of micro-failure, the ligamentary bridging mechanism is likely to occur, because longitudinal cells (tracheids/fibers) overlap rather than being arranged in linear longitudinal rows. The above implies that forms of energy dissipation other than surface energy are involved in wood crack propagation. These other forms are not accounted for in the LEFM.
7. The phenomenon called 'subcritical crack growth' is associated with crack propagation in a stable, quasi-static manner at values of K and G that are substantially below the critical values K_c and G_c (Atkinson and Meredith 1987). It is commonly related to systems subjected to long-term loading that causes delayed, static-fatigue failure. It is well known that the stability and rate of crack velocity can be controlled through appropriate choice of the rate of loading and experimental arrangement. Experimental evidence indicates that subcritical crack growth is characteristic of wood fracture behavior (Mai 1975; Yeh and Schniewind 1992).

Some recent research studies explicitly address the existence of an inelastic process zone ahead of the crack tip in wood. The application of J integral method (Yeh and Schniewind 1992) to single-edge notched Douglas-fir and Pacific madrone specimens revealed considerable differences between critical values of J_{Ic} and G_{Ic}, which are defined as equivalent in LEFM when material exhibits linear elastic behavior. The overall 'degree of plasticity' values (defined as relative differences between J_{Ic} and G_{Ic}) varied between 34 and 60% for Pacific madrone and 17 and 40% for Douglas-fir. The degree of plasticity increased for higher moisture contents (12, 18%, and green wood), higher temperature (70 to 140°F), and lower displacement loading rates (0.02 and 0.002 in./min). The general trends of the data

Note: N - non-linear zone

F - fracture process zone

L - linear zone

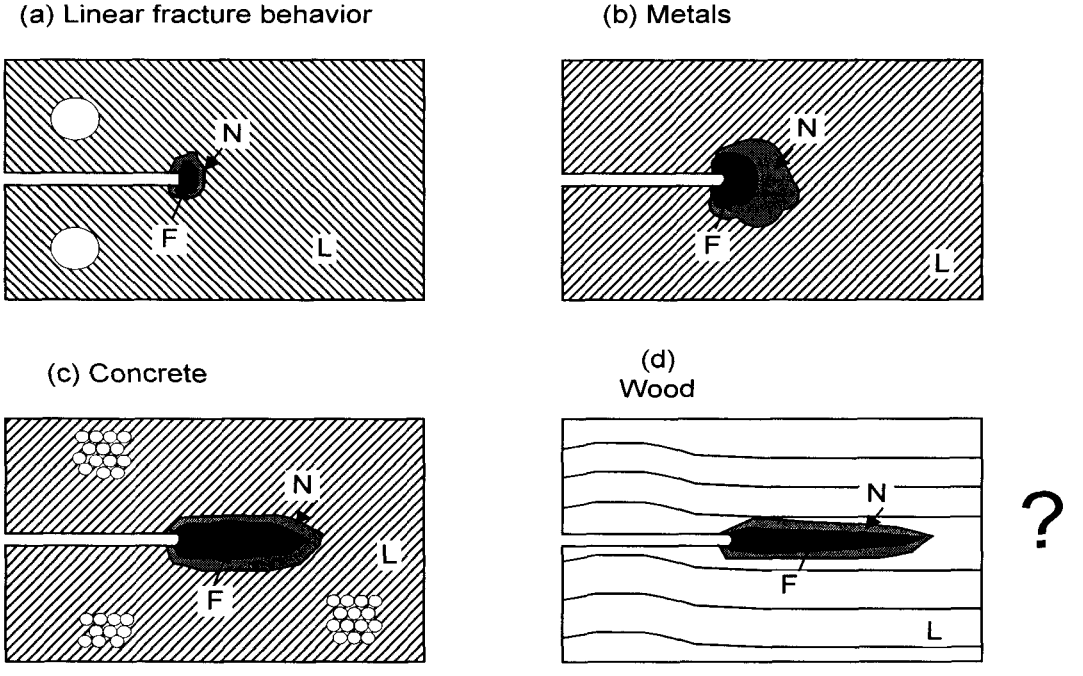

FIG. 1. Fracture process zone characterization.

appear to be in agreement with the issues previously discussed, but the designation plasticity is clearly incorrect for wood. There is no experimental evidence, or indication, that cracks in wood are accompanied by ductile, plastic deformations at room temperatures. Irreversible deformations, causing a certain amount of damage in wood ultrastructure, and apparently inelastic behavior in the crack fracture zone, are thought to be more appropriate descriptions for observed phenomena.

In respect to the overall LEFM approach, the criticism expressed above should not imply its general inapplicability to wood structures (the work by Smith et al. 1996 on notched beams shows the contrary). The most important issue is to determine when, how, and where in a structural member the conditions of the LEFM are prevailing, because if the scale conditions are met (and the fracture zone is sufficiently small), the LEFM should predict the same results as any nonlinear fracture model. Clearly, the more brittle the system, the greater the validity of LEFM. Several problems associated with somewhat strict LEFM applications to end-notched beams have been addressed by Smith and Springer (1993).

IN-SITU SEM STUDY (REAL-TIME OBSERVATIONS)

Based on the arguments expressed above, a study was undertaken to observe directly the

initiation and evolution of damage in the 'tip region' of cracks in wood. An experimental technique was developed based on facilities of the Scanning Electron Microscopy Unit at the University of New Brunswick's Fredericton campus.

The advent of powerful microscopic techniques has enabled post-mortem surface fractography to become a routine technique for characterization of fracture surfaces. However, post-mortem examinations enable limited understanding of fracture processes. Direct microscopic evidence of the evolution of steady-state crack propagation requires use of real-time *in-situ* scanning electron microscopy (Rodel et al. 1990). The objective of the work reported here was to identify the crack evolution including any restraining mechanisms due to bridging and micro-cracking at the crack tip. This implied the need for a test arrangement and specimen that favors subcritical stable, steady-state crack development.

A wedge-splitting test type device was designed for use in a JEOL JSM-6400 Scanning Electron Microscope, Figs. 2 and 3. The test method was chosen for its rather simple loading arrangement and ease of attachment to the existing SEM stage. Dimensions of the set-up and specimens were limited by the size of the SEM chamber and available working space. The wedge-splitting technique required a slender wedge to be inserted into a crack. The stage supporting the specimen was moved in the x-axis direction at a constant rate of displacement towards the stationary wedge.

An aluminum wedge was manufactured with a constant 'total' angle of 17°. The resultant degree of slenderness increased the stiffness of the specimen-loading set-up and ensured stability of the crack growth (ACI 446.1 R-91, 1991). The specimens were loaded by advancing the wedge at a constant speed of 3 mm/min. A load cell integral to the wedge facilitated measurement of load within the vacuum environment. It consisted of strain gauges attached at the end opposite to the point of the wedge, within the region of reduced cross-section.

Materials

All tests were carried out using eastern Canadian spruce (a combined group), previously kiln-dried and stored to stabilize the moisture content (MC) at 15%. For the SEM study, a discrete mesh was deposited over a sanded face by the vacuum vaporization technique for directional deposition of the gold coating. A 50-μm copper mesh was placed over the specimen prior to deposition, and its removal left a grid that facilitated measurement of the fracture process zone in the region of the crack tip. The grid was placed at 45° relative to the grain orientation, to ensure that the pattern did not coincide with the direction of the tracheids. The grid facilitated recognition and measurements of the extent of damage and crack profiles. Once the crack starts to open, it becomes highly visible due to edge charging of new crack faces. Care was exercised to reduce the effect of vacuum environment induced moisture content loss, which was seen not to cause any additional specimen damage.

Grain orientation and dimensions of the specimens

It is known that complete crack propagation and nonlinear fracture parameters can be obtained only if the crack velocity is controlled in such a manner that stable post-cracking response will ensue (Porter 1964). A favorable rate of change in compliance was accomplished by shaping the specimen in such a manner that it had an end-tapered DCB geometry, with outer dimensions shown in Fig. 2 and Table 1. The 0.5-mm-wide-notch was cut with a jewelry saw. Statistical significance of the data was beyond the scope of the study.

Choice of a small specimen thickness and selection of material with 'defect-free' ultrastructure were means of ensuring that the measurements and observations of cracks at the surface correlated well with the process in the interior of a specimen. An expected consequence was the introduction of a size-effect in measured fracture parameters, especially in terms of fracture energy G_f.

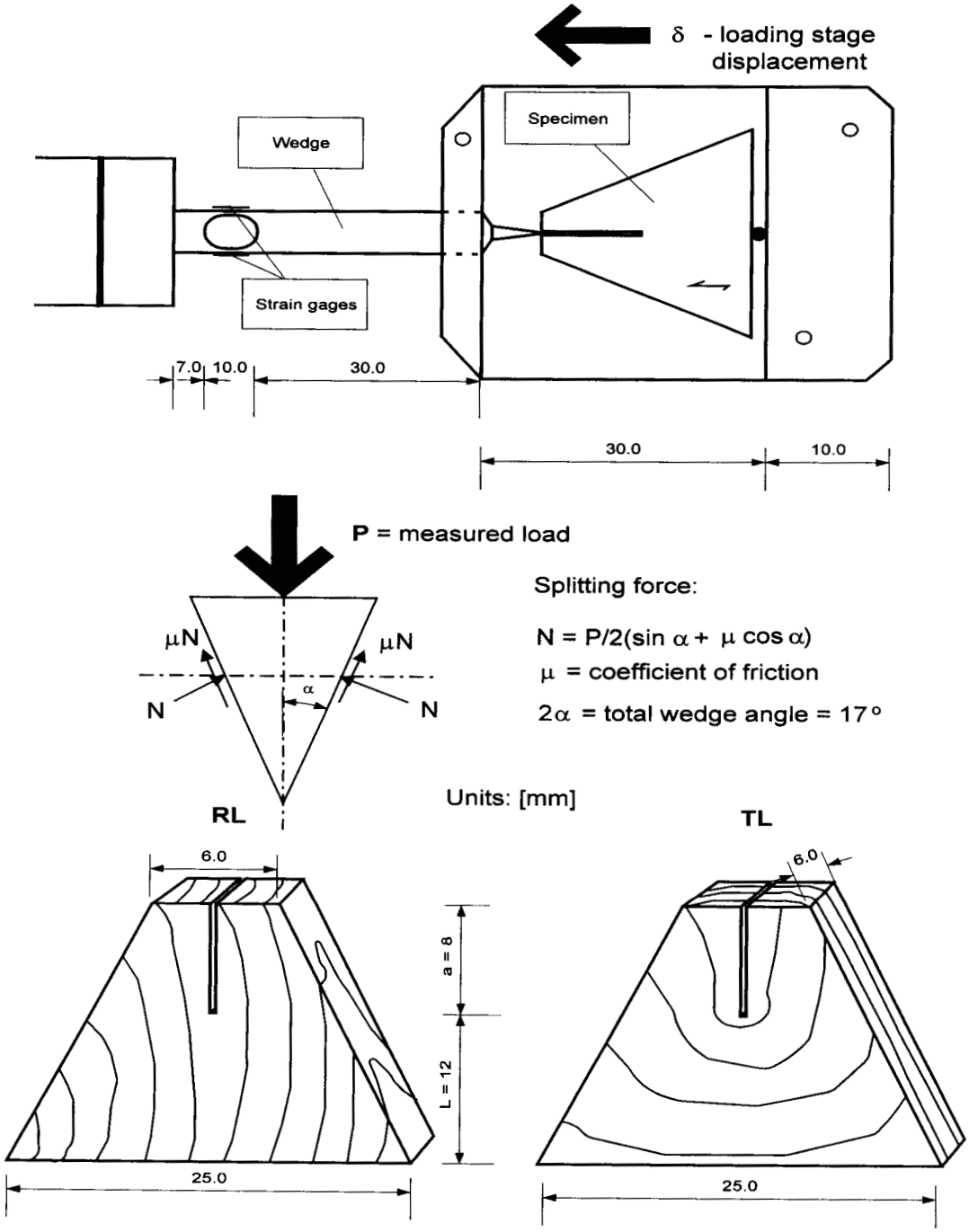

FIG. 2. Schematics of the wedge-splitting testing arrangement, dimensions, and orientations of the specimens (dimensions in [mm]).

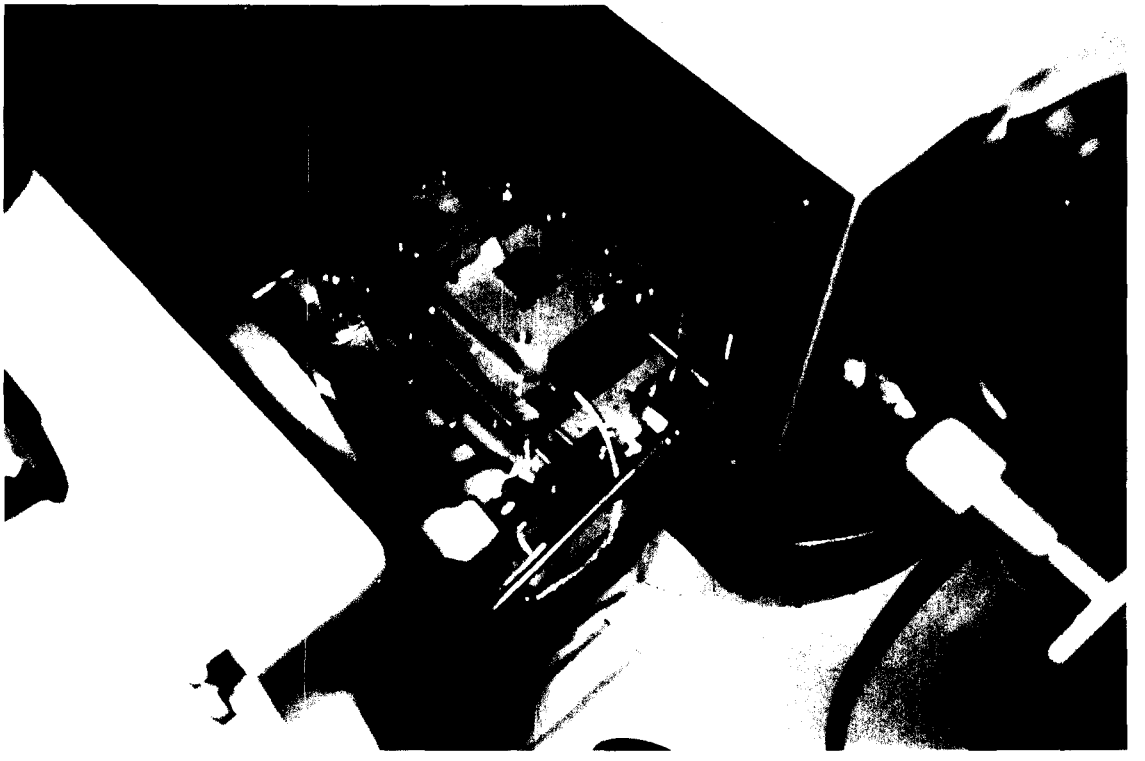

FIG. 3. Loading set-up in the SEM.

Evaluation of experimental data from SEM tests

With a loading rate of 3 mm/min, the time needed for complete fracture of the specimens was between 2 and 3 min. Wedge load versus time was recorded using a Sciemetric 200 data logging system. Accuracy of the manufactured wedge-load cell was estimated to be between 0.5 and 0.8% in the measuring range, calibrated against a 1 kN Instron load cell with an accuracy of 0.3% of the full range.

The process of crack evolution in real-time was videotaped. This allowed measurements to be made and crack profiles to be reconstructed.

TABLE 1. *Dimensions and orientations for end-tapered DCB specimens.*

Orientation	Thickness t [mm]	Notch length a [mm]	Ligament length l [mm]
RL (5)	6.2	7.9	12.1
TL (6)	5.7	7.8	12.3

Note: Values in the parentheses are the numbers of specimens in each of the series.

Qualitative SEM observations and characterization

Characteristic SEM micrographs showing 'restraining effects,' crack tips, and damage in the fracture process zone in the stable steady-state crack propagation regime are given in Figs. 4 to 13. Difficulties in correct identification of the crack tip, and thus, of the actual crack length are apparent in Figs. 4 and 5. After the first natural extension from the sharpened starter-notch, the load was applied intermittently to allow pictures to be taken in the 'still mode.' Under this fixed displacement, the crack would often continue to advance smoothly. The effect of local stress redistribution is related to time-sensitivity of the crack length during subcritical crack propa-

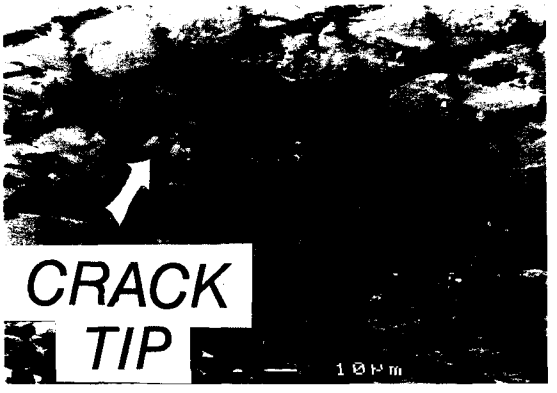

FIG. 4. SEM micrograph—crack tip, RL direction (load applied "R", crack propagates "L").

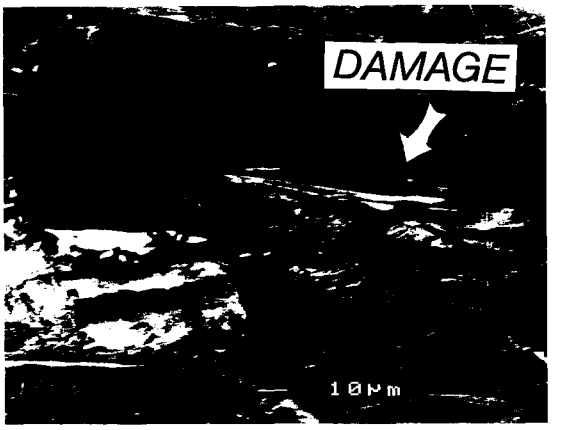

FIG. 6. SEM micrograph of fibers damage, RL direction.

gation. This short crack extension was strain-energy-driven and thus, self-arresting. Damage of fibers ahead of the crack tip, forming micro-cracks, is shown in Fig. 6.

Fiber bridging is shown in Fig. 7, while damage of the fibers at the crack tip towards the end of the test is shown in Fig. 8. Distortion of the grid along the opening crack is shown in Fig. 9.

Damage to the fibers in the RT direction is shown in Fig. 10. Some of the fibers are peeled off and some are broken. No consistency has been observed throughout the frac-

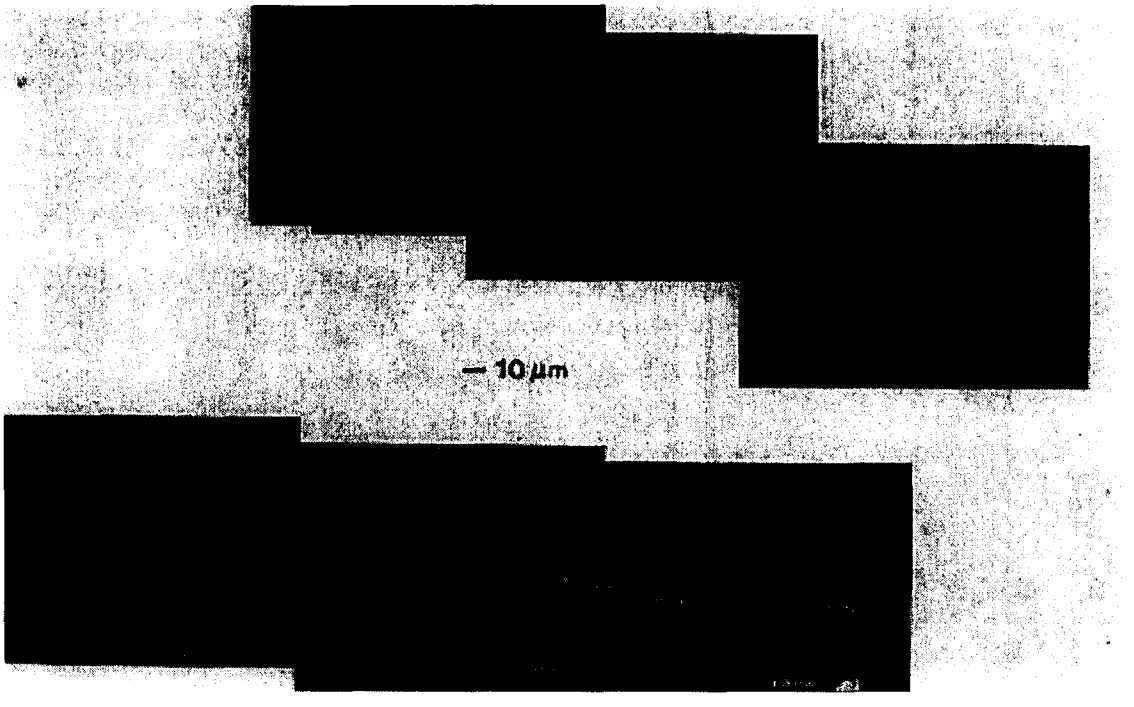

FIG. 5. Reconstruction of the SEM crack profiles from video-recordings, RL direction.

FIG. 7. SEM micrograph—fibers bridging, RL direction.

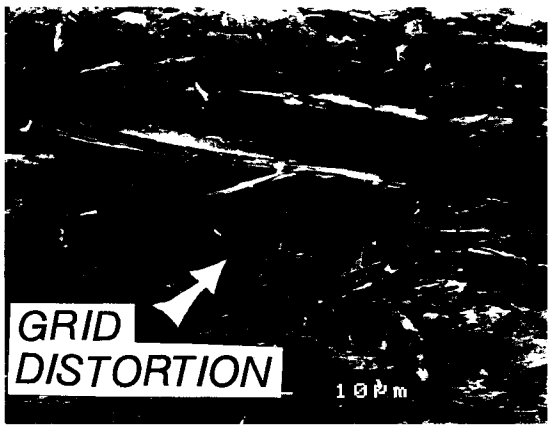

FIG. 9. SEM micrograph—distortion of grid on the surface.

turing process. Microcracks in the cell walls have been observed as shown in Figs. 11 to 13.

The initial crack extension from the notch tends to occur suddenly. Fracture response (i.e., load level and initial crack length) is influenced by the notch configuration and local material properties along the ligament that lies ahead of the notch.

Before the crack initiation, no damage could be detected on the surface of the specimen. Once initiated, the natural crack grows with a highly localized fracture zone in both length (1 to 2 mm) and width as measured on the specimen surface. Preexisting fine microcracks (i.e., flaws) were being opened close to the crack tip growing to more than 100 µm in length, while only those of critical size joined the main crack. This is primarily due to randomness of the interfacial cohesive strength within and between the cells (tracheids), i.e., intracell and intercell lateral cohesion. Some micro-cracks that formed in the damage zone were observed not to close completely when the major crack advanced, resulting in a finite residual strain behind the crack tip.

Presence of weak planes (i.e., low fracture energy interfaces) in close proximity to the tip causes the crack to deflect somewhat and leave

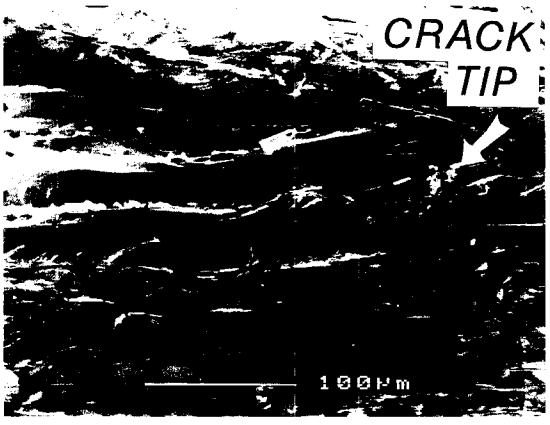

FIG. 8. SEM micrograph—fibers bridging and crack tip towards the end of test, RL direction.

FIG. 10. Fiber damage in the RT plane as the crack advances.

FIG. 11. Fiber peeling and bridging deformation due to crack growth.

FIG. 12. Micro-cracks in the cell walls.

a single fiber or bundles of fibers unruptured (Fig. 4). Intercellular micro-failures are beneficial for bridging effects. Whole fibers at first act as short beams between the cracks faces, and with further increase in load, the fibers either rupture at a small crack opening, or partial peeling off increases the span of fibers that deform in bending. Tensile stresses are highly localized in a short segment of the fibers, which often fail before any extension of the crack occurs. The exact contribution to toughness, from opening and extension of flaws, peeling off and closure forces due to bridging fibers, depends on the bridging configuration, which is not strictly self-repeating. Statistical experimental scatter of toughness and fracture energy measurements will thus reflect the differences in ultrastructure and the sequence of events along individual crack paths. *In-situ* crack interface observations under monotonic load indicate that in spruce stable crack advance involves opening, extension, and coalescence of the flaws or micro-cracks and subsequently fiber bridging. The crack never propagates in a strictly self-similar manner, due to the heterogeneous and discrete nature of the microstructure. Crack propagation in wood is locally episodic and is itself a heterogeneous process, with continuous reinitiation along the path of the crack. Although macroscopically it appears to be quasi-static growth, at the micro-scale phases of unstable rapid micro-failure alternate with phases of crack stability. Microscopically, fractured surfaces are irregular and tortuous. These observations pinpoint that the ability to transfer stress along the bridging zone makes it difficult to define a 'real crack tip' during its episodic advance.

Bridging is the main mechanism of crack-tip shielding in spruce, causing reduction of the stress tip singularity. This is because cells (tracheids) overlap rather than being arranged in linear longitudinal rows. There is no evidence of a large zone with micro-cracks ahead of the crack tip, as occurs in concrete, rocks, and ceramics.

Quantitative fracture zone characterization—bridging stresses from crack profiles

Quantitative damage zone characterization is presented in terms of measured crack pro-

FIG. 13. Micro-cracks in the cell walls.

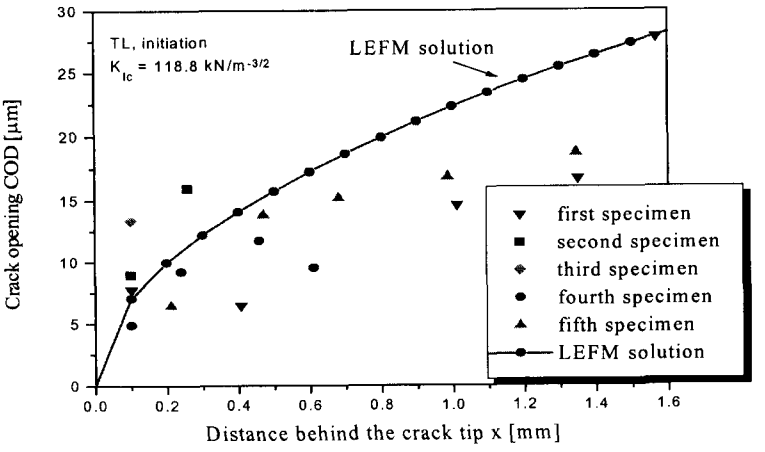

(a)

initiation

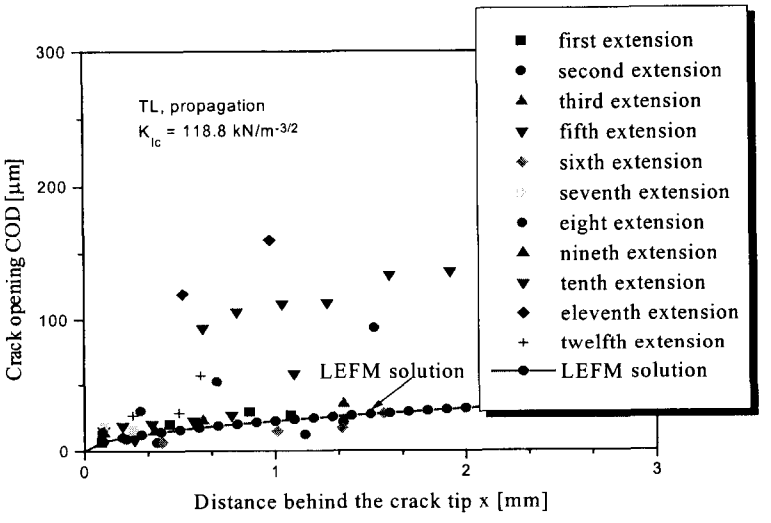

(b)

propagation

FIG. 14. Crack profiles in TL direction a) initiation b) propagation (5 replicates).

files. As expected, wood fracture behavior deviates from the ideal LEFM response. This is apparent from visible deviations of crack profiles from those associated with LEFM. The crack profiles were reconstructed from the video-recordings for the TL and RL fracture directions, with a resolution of measurements better than 1 μm. Resolution is dictated by use

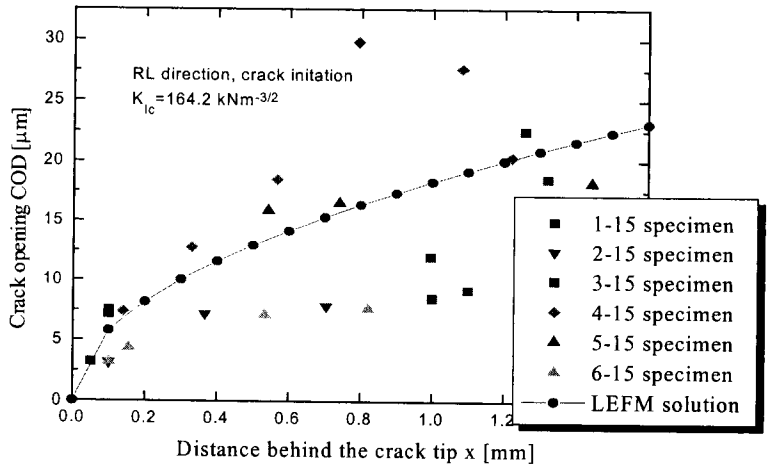

(a)

initiation

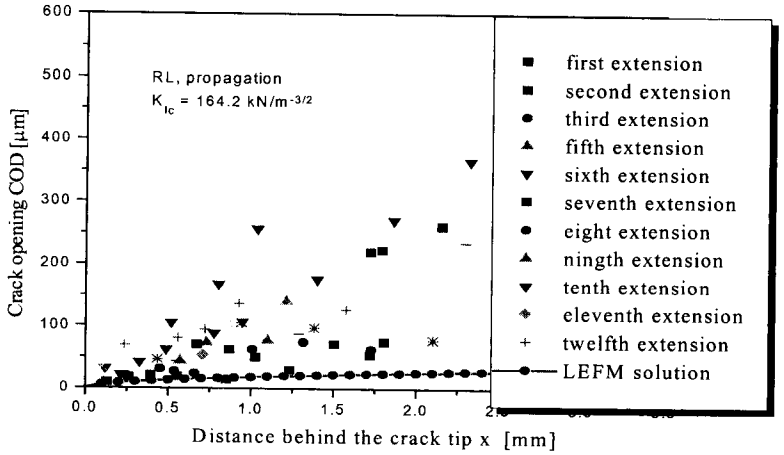

(b)

propagation

FIG. 15. Crack profiles in RL direction a) initiation b) propagation (6 replicates).

TABLE 2. *Summary of the results obtained in the SEM, RL direction.*

Specimen #	Max. load P_{max} [N]	P_{Max} per t P/t [N/mm]	Fracture toughness K_{IC} [kNm$^{-3/2}$]	Energy release G_{IC} [N/m]	Fracture energy G_f [N/m]
1–15	30.88	5.16	221.0	59.7	91.9
2–15	13.47	2.23	97.9	11.9	53.1
3–15	26.61	4.51	197.0	48.4	83.6
4–15	18.0	3.56	170.4	36.1	51.5
5–15	20.64	3.31	134.9	22.6	40.7
Mean	21.92	3.75	164.2	35.7	64.2
STD	6.18	1.01	43.8	17.2	19.9
COV	0.282	0.269	0.267	0.482	0.310

of a low acceleration voltage (2 kV) during the real-time fracturing. This was necessary to reduce edge charging of crack interfaces while maintaining sharp images of crack profiles. Because of irregular fracture surfaces across the thickness, crack faces on the surface of the specimen were not always well-defined. Data for initiated and propagating cracks are shown in Figs. 14 and 15 for the TL and RL directions, respectively. Crack Opening Displacements (COD) at crack interfaces are plotted as a function of distance behind the crack tip. Although there exists a scatter in measured values of Crack Opening Displacement (COD) in both directions, conclusions are drawn based on the apparent trend and deviations from the LEFM solution. Measured values are compared to the theoretical solutions for cracks in an infinite body (Sih et al. 1965) in order to estimate the extent of discrepancies.

Theoretical solutions for crack openings are evaluated based on mean measured values of fracture toughness in the SEM tests: K_{Ic} = 164.2 (STD 43.8) kNm$^{-3/2}$ in the RL direction (Table 2) and K_{Ic} = 118.8 (STD 31.4) kNm$^{-3/2}$ in the TL direction (Table 3).

A simple method for evaluation of bridging stresses from measured crack profiles is illustrated using the measured data from fracture of RL specimen 4–15 (Table 2). A parabolic crack profile that corresponds to the theoretical stress-free LEFM is shown in Fig. 15 as a solid line. Crack profiles for the LEFM case were obtained using Finite Element analysis (Vasic 2000). Critical stress intensity factor of K_{Ic} = 170.4 kNm$^{-3/2}$ (Table 2) is calculated from the maximum peak load P_{max}. The values of fracture toughness and fracture energy given in Tables 2 and 3 are intended to provide basic Linear and Non-linear Elastic Fracture Mechanics parameters of tested specimens.

Close examination of the results showed that the first extension of the natural crack from the rectangular starter-notch exhibits a crack profile, which is very close to the LEFM solution. Further extension of the 'natural' crack involves both crack propagation and separation of the crack faces, and crack resis-

TABLE 3. *Summary of the results obtained in the SEM, TL direction.*

Specimen #	Max. load P_{max} [N]	P_{Max} per t P/t [N/mm]	Fracture toughness K_{IC} [kNm$^{-3/2}$]	Energy release G_{IC} [N/m]	Fracture energy G_f [N/m]
1–17	11.66	1.87	105.0	10.1	17.2
2–17	11.69	1.89	108.9	10.8	26.9
3–17	13.7	2.18	120.2	13.2	33.5
4–17	7.97	1.68	107.1	10.4	25.1
5–17	6.13	1.28	86.3	6.5	11.0
6–17	12.95	2.64	185.5	29.3	54.8
Mean	10.68	1.92	118.8	13.4	28.1
STD	2.72	0.42	31.4	7.4	13.1
COV	0.255	0.218	0.264	0.552	0.466

tance is high compared to the LEFM assumption of constant fracture toughness along the fracture plane. Crack profiles for the subsequent crack extension (l = 5.8 mm), measured from the videotape of crack propagation, correspond to the stress intensity factor of K_{Ic} = 220 kNm$^{-3/2}$. The parabolic shape of the CODs profile is not influenced significantly by bridging stresses. Shape of the opening mechanism changes when the crack is approaching the end of the specimen (l = 11.3 mm). The crack profile becomes linear, and the mechanism of crack advance indicates strong deviations from the LEFM solution. Fracturing in the TL direction exhibits a similar apparent trend of crack profiles evolution as noted for the RL direction (Fig. 14).

CONCLUSIONS

This paper deals with micro-mechanical aspects of wood fracture and specifically the fracture zone in spruce. A real-time *in-situ* SEM study was necessary to establish the nature of deviations, for wood, from an ideal brittle response as presumed by the LEFM approach. Conclusions drawn from the work presented are:

1. At the micro-scale, and when using small size specimens, wood fracture behavior should be considered as nonlinear. The basic assumptions of LEFM do not hold.
2. Because of the heterogeneous and fibrous nature of the micro-structure, fiber bridging is the main toughening mechanism during crack propagation in spruce loaded in the TL or RL direction. There is no extensive fracture zone ahead of a crack tip, as is assumed in cohesive (fictitious) crack models (Bostrom 1992). Bridging causes crack profiles, and thus fracture toughness, to deviate significantly from those predicted by LEFM.
3. Initiation of cracks using a wedge-splitting apparatus occurs suddenly at the maximum peak load, without previous visible surface damage.
4. Although moisture content of wood decreases significantly in a vacuum environment during a test, this does not invalidate the phenomenological conclusions about the fracture mechanisms of fibers bridging and failure patterns.
5. As a 'rough estimate', characteristic fracture parameters (i.e. fracture toughness, energy release rate, and fracture energy) deviate from LEFM values between 10 and 30%. The difference is the contribution of bridging stresses along the crack faces to the net tip fracture toughness and fracture energy.

NOTATION.

a^o	= intrinsic flaw size
COD	= crack opening displacement
δ	= deformation
G_f	= specific fracture energy
G_{IC}	= energy release rate (mode I)
G_b	= bridging fracture energy
K_{Ic}	= fracture toughness (mode I)
RL	= radial longitudinal direction (stress in R direction, crack growth in L direction)
TL	= tangential longitudinal direction (stress in T direction, crack growth in L direction)

ACKNOWLEDGMENTS

The authors express gratitude to the following technical staff from the University of New Brunswick: Mr. J. Barns for help with Scanning Electron Microscopy tests, Mr. D. Wheaton for manufacturing the loading device, and to Mr. D. McCarthy for manufacturing the specimens. Funding was received from the Natural Sciences and Engineering Research Council of Canada (NSERC).

REFERENCES

ACI 446.1 R-1. 1991. Fracture mechanics of concrete: Concepts, models, determination of material properties. Report by American Concrete Institute Committee, 446, Detroit, MI. 108 pp.

ASHBY, M. F., F. R. S. EASTERLING, R. HARRYSON, AND S. K. MAITI. 1984. The fracture and toughness of wood. Report, Cambridge University, Dept. of Engineering, Cambridge, UK. 82 pp.

ATKINSON, B. K. 1987. Introduction to fracture mechanics and its geophysical applications. pages 1–27 *in* B. K.

Atkinson, ed. Fracture mechanics of rocks. Academic Press Ltd., London, UK.

———, AND P. G. MEREDITH. 1987. The theory of subcritical crack growth with application to minerals and rocks. pages 58–77 *in* B. K. Atkinson, ed. Fracture mechanics of rocks, Academic Press Ltd., London, UK.

ATTACK, D., W. D. MAY, E. L. MORRIS, AND R. N. SPROULE. 1961. The energy of tensile and cleavage fracture of black spruce, Tappi 44(8):555–567.

BOSTROM, L. 1992. Method for determination of the softening behavior of wood and applicability of a non-linear fracture mechanics model, Report TVBM—1012, Lund University, Lund, Sweden.

BROEK, D. 1982. Elementary engineering fracture mechanics. Martinus Nijhoff Publishers, The Hague, The Netherlands.

KNOTT, J. F. 1973. Fundamentals of fracture mechanics. Butterworth & Co., London, UK.

MAI, Y. W. 1975. On the velocity-dependent fracture toughness of wood. Wood Science 8(1):364–367.

PORTER, A. W. 1964. On the mechanics of fracture in wood. Forest Prod. J., 14(8):325–331.

RODEL, J., J. F. KELLY, AND B. R. LAWN. 1990. *In situ* measurements of bridged crack interfaces in the scanning electron microscope. J. Am. Ceramic Soc. 73(11): 3313–3318.

SIH, G. C., P. C. PARIS, AND G. R. IRWIN. 1965. On cracks in rectilinear anisotropic bodies. Int. J. Fracture 1:189–203.

SMITH, I., AND G. SPRINGER. 1993. Consideration of Gustafsson's proposed eurocode 5 failure criterion for notched timber beams. Can. J. Civil Eng. 20(6):1030–1036.

———, AND Y. H. CHUI. 1994. Factors affecting mode I fracture energy of plantation-grown red pine, Wood Sci. Technol. 28:147–157.

———, AND L. J. HU. 1994. Fracture analysis of bolted connections, American Society of Civil Engineers Structural Congress XII, April 25–28, Atlanta, GA, 2: 912–917.

———, D. M. TAN, AND Y. H. CHUI. 1996. Critical reaction forces for notched timber members, International Wood Engineering Conference '96, New Orleans, October 28–31, Louisiana State University, Baton Rouge, LA, 3.460–3.466.

VALENTIN, G. H., L. BOSTROM, P. J. GUSTAFSSON, A. RANTA-MAUNUS, AND S. GOWDA. 1991. Application of fracture mechanics to timber structures, RILEM State-of-the-art report, Technical Research Centre of Finland, Research Notes, 1262. Espoo, Finland.

VASIC, S. 2000. Applications of fracture mechanics to wood. Ph.D. thesis, University of New Brunswick, Fredericton, New Brunswick, Canada.

———, AND I. SMITH 1996a. On the influence of ultrastructure and fibres bridging in mode I fracture of wood, Proc. 2nd International Conference on the Development of Wood Science/Technology and Forestry ICWSF'96, April 10–12, University of Sopron, Sopron, Hungary.

———, AND ———. 1996b. The brittleness of wood in tension perpendicular to the grain: Micro-mechanical aspects. International COST 508 Wood Mechanics Conference, May 14–16, Stuttgart. Office of Publications of the European Communities, Luxembourg: pp. 555–569.

———, AND ———. 1998. Bridged crack model of wood fracture: Experimental analysis and numerical modeling, Proc. World Timber Engineering Conference, August 17–20, Montreux, Swiss Federal Institute of Technology, Lausanne, Switzerland. 1.818–1.819.

———, AND ———. 1999. The effect of bridging stresses on fracture toughness of wood, RILEM Symposium on Timber Engineering, Sweden, 13–15 September, Stockholm.

YEH, B., AND A. P. SCHNIEWIND. 1992. Elasto-plastic fracture mechanics of wood using the J-integral method. Wood Fiber Sci. 24(3): 364–376.